Biophysical Chemistry 143 (2009) 26–33

Contents lists available at ScienceDirect

Biophysical Chemistry

journal homepage: http://www.elsevier.com/locate/biophyschem

Characterization of cooperative effects in linear α-glycylglycine clusters

Aidin Bahrami, Mehdi D. Esrafili, Nasser L. Hadipour *

Department of Chemistry, Tarbiat Modares University, Tehran, Iran

ARTICLE INFO

Article history:
Received 21 December 2008
Received in revised form 16 March 2009
Accepted 20 March 2009
Available online 5 April 2009

Keywords:
Hydrogen-bonding cooperativity
DFT
Glycylglycine
NMR
Atoms in Molecules analysis

ABSTRACT

The aspects of N–H···O═CNH, N–H···O═CO and C–H···O═CNH interactions are analyzed by applying ab initio and DFT methods as well as Bader theory. We investigated geometry, binding energies, ^{17}O, ^{15}N chemical shift tensors, and Atoms in Molecules (AIM) properties of α-glycylglycine (α-glygly) clusters, via MP2, B3LYP and $PW91_{XC}$ methods. Dimer stabilization energies and equilibrium geometries are studied in various levels of theory. MP2 and DFT calculations reveal that for α-glygly clusters, stability of N–H···O and C–H···O hydrogen bonds are enhanced significantly as a result of cooperativity effects. Furthermore, a covalent nature is also detected for some hydrogen bondings. The *n*-dependent trend of ^{17}O and ^{15}N chemical shift tensors was reasonably correlated with cooperative effects in hydrogen-bond interactions. Regarding the various N–H···O═CNH, N–H···O═CO and C–H···O═CNH hydrogen bondings, capability of the α-glygly clusters for electron localization at the N–H···O and C–H···O bond critical points, depends on the cluster size. This leads to cooperative changes in the hydrogen-bond length and strength as well as ^{17}O and ^{15}N chemical shift tensors.

1. Introduction

It is becoming increasingly apparent that many-body (or cooperative) effects in intermolecular interactions play an important role in the modern view of condensed matter [1]. Since the equations of classical electrostatic include only pair-wise additive interactions of localized monomers, the existence of these effects can be considered as a departure from the classical electrostatic model of hydrogen bonding (H-bonding), indicating the inadequacy of considering its electrostatic picture alone, and, perhaps even more important, suggesting the presence of significant electronic delocalization [2–6]. Various physical and chemical properties are influenced by cooperativity effects, including geometry, binding energy, vibrational and nuclear magnetic resonance (NMR) properties [5–14]. For example, secondary and tertiary structures of biomolecules and related assemblies may be stabilized due to the cooperativity effect. Dannenberg et al. [15] reported an unusually high degree of cooperativity in hydrogen-bond chains of formamide and their implications in protein modeling. They also indicated that cooperativity effects play an important role in energetics of the association of β-strands form β-sheets [16]. Kar and Scheiner [17] have just recently conducted a comparative study between the cooperativity in C–H···O and O–H···O hydrogen bonds. Rather interesting results are found revealing that although cooperativity of the C–H···O and O–H···O bonds is similar, solvent effects, represented by a continuum with a dielectric constant, may reduce cooperativity in all systems.

It is well-known that there are two kinds of cooperativity in H-bonding theory [18]. The first one is connected with π-electron delocalization, and resonance assisted hydrogen-bonded (RAHB) systems. The second kind is related to σ-bonds connected to each other via a chain or a cycle. Species with N–H···O interactions, i.e., O═CNH···O═CNH···O═CNH between the chains are suitable examples. Such a situation often occurs in crystals where the subsystem is reduplicated within the chains in line with the translational symmetry required. Influence of the cooperative effects on the H-bond properties was investigated recently using experimental microwave and theoretical techniques for $H_3N{\cdots}HF$ and $H_3N{\cdots}HF{\cdots}HF$ complexes [19]. It is found that addition of the second HF molecule to the $H_3N{\cdots}HF$ complex leads to a 0.21(6) Å reduction in the N···H hydrogen bond. In other words, the cooperativity effect exists in clusters where the monomer can participate concertedly as donor and acceptor. There are also numerous theoretical investigations on the cooperativity effect [20,21]. For example, cooperativity in N–H···O═CNH hydrogen bond in benzamide [22] and acetamide [23] was investigated. Results indicated that cooperative effects enhance the H-bond strength and decrease the covalent nature of the proton donating bond. The effects are evidenced as elongation and a red shift in the corresponding stretching mode. In case of acetamide, cooperativity down-shifting was detected for calculated ^{14}N nuclear quadrupole coupling constants (NQCCs). There are other types of H-bonds, for example C–H···F, where an enhancement of blue shift is observed as a result of cooperativity [24]. Cooperativity may exist for different kinds of hydrogen bonds, so-called conventional and unconventional ones.

* Corresponding author. Tel.: +98 2188011001 3495; fax: +98 218800 9730.
E-mail address: hadipour@modares.ac.ir (N.L. Hadipour).

0301-4622/$ – see front matter © 2009 Elsevier B.V. All rights reserved.
doi:10.1016/j.bpc.2009.03.011

There are very interesting π-hydrogen-bonded interactions analyzed at the MP2/6-311++G(2d,2p) level of approximation [25]. The other example where the H-bond cooperativity analyzed for chains of acetic acid molecules [26] is a very important contribution. It is found that a rather small cooperativity, 1.2 kcal/mol (at the HF/6-31G** level of theory), is present along the acetic acid molecules.

A number of theoretical investigations have been performed concerning cooperative effects on structural and spectroscopic parameters of H-bonds in model peptides [27,28]. However, little information is available for the biologically important O═CNH···O═CNH and N–H···O═CO groups. α-Glycylglycine (α-glygly) looks like a simple molecular model for the presence of the cooperative effects in the O═CNH···O═CNH and N–H···O═CO interactions. Owing to the importance of these interactions in proteins and polypeptides stability, α-glygly has received most attention from theoretical [29–31] and experimental [32–36] points of view. Although the importance of H-bonding interactions in crystalline structure of α-glygly has been previously shown [31], the investigations on the cooperative effects of α-glygly clusters have not been done from survey. The present work is designed to theoretically address H-bonding cooperativity for linear crystalline α-glygly clusters in a systematic manner. In addition to the energetics, calculations address the lengths of the H-bonds, including perturbations induced in the internal geometry of each monomer. Spectroscopic aspects of the interactions are considered as well, in particular the NMR chemical shift isotropy and anisotropy parameters of relevant nuclear centers. We also focus on the electron density redistribution, induced by hydrogen-bond formation, and its variation by increasing the units in the chain. Topological parameters, such as total energy density (H_C) and Laplacian of electron density at bond critical point ($\nabla^2\rho_C$), are useful to classify the covalent nature of interactions. Thus, the topic of covalency for cooperative H-bonded interactions is also discussed.

2. Methods of calculations

2.1. MP2 and DFT calculations

Molecular orbital calculations were performed using DFT and MP2 methods. All the computations were carried out using Gaussian 98 program [37]. A personal computer with a 3 GHz Pentium IV processor and 1024 MB of RAM was used for computations. The geometry optimization of monomer and dimer α-glygly was performed using the B3LYP, $PW91_{XC}$ and MP2 methods with 6-31+G*, 6-31++G**, cc-pVDZ and aug-cc-pVDZ basis sets. For geometry optimization of linear $(\alpha\text{-glygly})_{3-5}$ clusters, the B3LYP method with 6-31+G* basis set is applied (Fig. 1). Although, it has been extensively shown that counterpoise-correction (CP) [38] is necessary for obtaining correct geometries of H-bonding clusters [39]. However, the $(\alpha\text{-glygly})_{1-5}$ geometries were not optimized on the CP surface as a result of CPU time limitations. Only the interaction energies obtained at the MP2 and DFT levels were corrected for the basis set superposition error (BSSE) [38]. The BSSE corrected energies were determined as

$$\Delta E = E_n - \sum_i^n E_i \tag{1}$$

where E_n is the total energy of the cluster of size n, and E_i is the energy of the individual monomers, in the cluster geometry, calculated using all the basis set of the cluster. According to the results presented by Novoa and Sosa [40], MP2 correlation method provides a better description of the energetics of H-bonded complexes than DFT methods.

^{17}O and ^{15}N chemical shift calculation was computed using gauge-including atomic orbital (GIAO) approach [41] at the B3LYP/6-311++G** level of theory. The method has been to produce rather accurate data for hydrogen-bonded systems [42,43]. The principal components calculated using chemical shift tensor ($\sigma_{11} \le \sigma_{22} \le \sigma_{33}$) were applied to compute the chemical shift isotropy, σ_{iso}, and anisotropy, $\Delta\sigma$, parameters. These parameters are defined as [44]:

$$\sigma_{iso}(\text{ppm}) = \frac{\sigma_{11} + \sigma_{22} + \sigma_{33}}{3} \tag{2}$$

$$\Delta\sigma(\text{ppm}) = \sigma_{33} - \left(\frac{\sigma_{11} + \sigma_{22}}{2}\right). \tag{3}$$

Since quantum chemical calculations yield absolute chemical shift values, one must establish the absolute shift values for a particular nucleus to obtain a direct relation between the calculated results and experimentally reported data. To evaluate the chemical shift tensor components, δ_{ii}, from the calculated $\sigma_{ii,cal.}$ values, we used

$$\delta_{ii,} = \sigma_{ii,ref.} - \sigma_{ii,cal.}$$

where $\sigma_{ii,ref}$ refers to the absolute chemical shift of liquid water and liquid ammonia with the $\sigma_{iso,ref}$ = 287.50 and 244.6 ppm, respectively [45,46].

2.2. Atoms in Molecules (AIM) calculations

AIM analysis was performed using AIM 2000 code [47]. For atom–atom interactions such as intermolecular contacts or valence bonds, the characteristics of the corresponding bond critical point (BCP) are very important [48] for determination of electron density (ρ_C) and its Laplacian ($\nabla^2\rho_C$). The energetic properties of BCPs are often considered as the electron energy density at BCP (H_C) and its components: the kinetic electron energy density (K_C) and the potential electron energy density (V_C). There is a relation between these energetic characteristics, $H_C = K_C + V_C$. It is also known from the

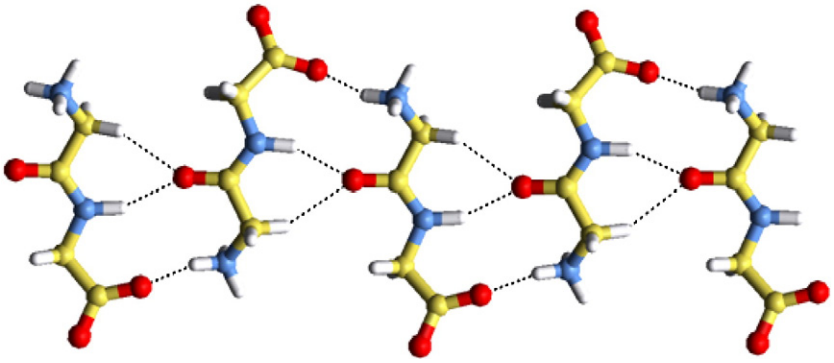

Fig. 1. Hydrogen-bonding network of $(\alpha\text{-glygly})_5$ cluster optimized at B3LYP/6-31+G* level.

Table 1
Calculated structural properties of monomer and dimer α-glygly[a].

Parameter	Method	6-31+G*	6-31++G**	cc-pVDZ	aug-cc-pVDZ
Monomer					
r_{N-H}	B3LYP	1.0193	1.0183	1.0210	1.0207
	$PW91_{XC}$	1.0279	1.0267	1.0313	1.0269
	MP2	1.0214	1.0189	1.0216	1.0210
$r_{C=O}$	B3LYP	1.2435	1.2410	1.2498	1.2415
	$PW91_{XC}$	1.2540	1.2518	1.2620	1.2532
	MP2	1.2468	1.2411	1.2449	1.2531
r_{C-N}	B3LYP	1.3313	1.3310	1.3353	1.3342
	$PW91_{XC}$	1.3407	1.3403	1.3406	1.3404
	MP2	1.3303	1.3301	1.3327	1.3319
Dimer					
r_{N-H}	B3LYP	1.0216	1.0209	1.0231	1.0221
	$PW91_{XC}$	1.0320	1.0312	1.0348	1.0316
	MP2	1.0264	1.0251	1.0279	1.0262
$r_{C=O}$	B3LYP	1.2535	1.2531	1.2518	1.2501
	$PW91_{XC}$	1.2638	1.2630	1.2695	1.2629
	MP2	1.2520	1.2517	1.2565	1.2552
r_{C-N}	B3LYP	1.3242	1.3225	1.3270	1.3252
	$PW91_{XC}$	1.3330	1.3326	1.3351	1.3332
	MP2	1.3281	1.3277	1.3291	1.3240
$r_{N-H\cdots O=CNH}$	B3LYP	2.1696	2.1617	2.1685	2.1624
	$PW91_{XC}$	2.1348	2.1322	2.1364	2.1326
	MP2	2.0981	2.0814	2.0917	2.0903
$r_{N-H\cdots O=CO}$	B3LYP	1.6475	1.6360	1.6959	1.6823
	$PW91_{XC}$	1.6645	1.6606	1.7222	1.7194
	MP2	1.6601	1.6441	1.7011	1.6942
$r_{C-H\cdots O=CNH}$	B3LYP	2.4898	2.4818	2.5070	2.4972
	$PW91_{XC}$	2.6046	2.6023	2.6157	2.6061
	MP2	2.5912	2.5991	2.6091	2.5945

[a] Distances in angstroms.

virial theorem that $1/4\nabla^2\rho_C = 2K_C + V_C$. The negative value of the Laplacian of the electron density at BCP designates the concentration of the electron charge among the nuclei of interacting atoms and is typical for covalent bonds-shared interactions. In some studies it is also stated that for $\nabla^2\rho_C > 0$ and $H_C < 0$, the interaction may be regarded as partly covalent in nature. For positive values of $\nabla^2\rho_C$, there is a depletion of electron charge between the atoms, indicating an interaction of closed-shell systems: ions, van der Waals interactions or H-bonds. Hence, the Bader theory arbitrarily provides the characteristics of BCPs depending on the covalent nature of interaction.

3. Results and discussion

3.1. Analysis of structural parameters

Glygly is composed of two glycine residues; however, in the solid state, it forms three different polymorphs, designated as α, β and γ by Bernal [49]. In crystalline structure, α-glygly presents three types of intermolecular interaction: N–H···O═CNH, N–H···O═CO, and a weak C–H···O═CNH type. The arrangement of molecules within each layer resembles the anti-parallel β-sheet motif observed in proteins; in α-glygly the motif is constructed through NH···O═CNH hydrogen bonds rather than covalent amid link.

The calculated structural parameters for monomer and dimer α-glygly using the DFT and MP2 methods at the 6-31+G*, 6-31++G**, cc-pVDZ and aug-cc-pVDZ basis sets are presented in Table 1. For the monomer α-glygly, a general comparison reveals that all calculated bond distances are slightly longer than the experimental values obtained for α-glycine from microwave study ($r_{N-H} = 1.01$ Å) [50]. Furthermore, for a given method, addition of the diffuse and polarization functions into the basis set produces no significant influence in geometrical parameters. A similar result is obtained for linear chains of formamide [51] and acetamide [23] molecules, in which a variety of basis sets at MP2 and DFT levels were employed. The $r_{C=O}$ and r_{C-N} bond distances obtained from 6-31++G** basis set are found to be lower, compared to other theoretical methods at different basis sets.

Surveying the calculated results using the DFT and MP2 methods at different basis set levels reveals that changes in the monomer geometry are relatively considerable upon dimer formation. As in Table 1, a small elongation in the N–H and C═O bonds, involved in hydrogen bond, and a very slight contraction in C–N bond distance are evidenced as dimer molecules are produced. A similar trend is present for other systems involving N–H···O═CNH hydrogen bond [23,27,28,51]. Among all the applied theoretical methods, MP2 gives the maximum r_{N-H} length change, ca. 0.0050–0.0062 Å, at the four basis set levels. The main difference between the results provided by various methods was observed in the intermolecular distance between the atoms involved in hydrogen bond. The N–H···O═CNH distance is decreased at all basis set levels (with B3LYP>$PW91_{XC}$>MP2 order). Thus, with the aug-cc-pVDZ, the P3LYP method provides distances about 0.0721 Å longer than those obtained with the MP2 method, and the $PW91_{XC}$ method gave intermediate values. On the other hand, addition of diffuse and polarization functions to the 6-31+G* and cc-pVDZ basis sets shortens N–H···O═CNH, N–H···O═CO, and C–H···O═CNH distances.

As in Table 2, cooperative effects lead to interesting geometries for the different α-glygly clusters. Geometry changes are more prominent for interior molecules, reflecting the considerable influence of cooperative effects. According to our results, all of the N–H bonds acting as H-donors and the C═O bonds acting as H-acceptors are almost elongated relative to the isolated α-glygly molecule (1.019 Å). The calculated r_{N-H} and $r_{C=O}$ distances for pentamer cluster are given as follows: (1.023, 1.024, 1.025, 1.025, 1.028 Å) and (1.245, 1.246, 1.246, 1.247, 1.248 Å), respectively. On the other hand, a regular decrease in r_{C-N} is generally observed upon cluster enlargement from dimer to pentamer. The relation between average $r_{C=O}$ and r_{N-H} bond distances in the linear α-glygly clusters is obtained by (Fig. 2):

$$r_{C=O} = 0.939 r_{N-H} + 0.282 \quad \left(R^2 = 0.964\right) \tag{4}$$

which suggests the C═O bond order to be correlated with an increase in N–H bond distance. The *n*-dependence variations in either N–H and

Table 2
Structural parameters for $(\alpha\text{-glygly})_{1-5}$ optimized at B3LYP/6-31+G* level[a].

Parameter	$n=1$	$n=2$	$n=3$	$n=4$	$n=5$	Exp.[b]
r_{N-H}	1.019	1.022	1.024	1.024	1.025	0.090
		1.025	1.024	1.024	1.025	
			1.028	1.023	1.024	
				1.028	1.023	
					1.028	
$r_{C=O}$	1.243	1.243	1.245	1.245	1.246	1.228
		1.253	1.242	1.247	1.248	
			1.251	1.246	1.246	
				1.247	1.247	
					1.245	
r_{C-N}	1.331	1.328	1.328	1.326	1.326	1.326
		1.324	1.328	1.326	1.326	
			1.321	1.326	1.326	
				1.326	1.326	
					1.326	
$r_{N-H\cdots O=CNH}$	–	2.170	1.978	1.977	1.977	2.091
			1.932	1.958	1.968	
				1.980	1.960	
					1.980	
$r_{N-H\cdots O=CO}$	–	1.907	1.717	1.711	1.718	1.908
			1.905	1.825	1.717	
				1.909	1.713	
					1.913	
$r_{C-H\cdots O=CNH}$	–	2.490	2.404	2.404	2.404	2.413
			2.488	2.404	2.404	
				2.420	2.416	
					2.425	

[a] Distances in angstroms.
[b] Experimental values for crystalline α-glygly from Ref. [32].

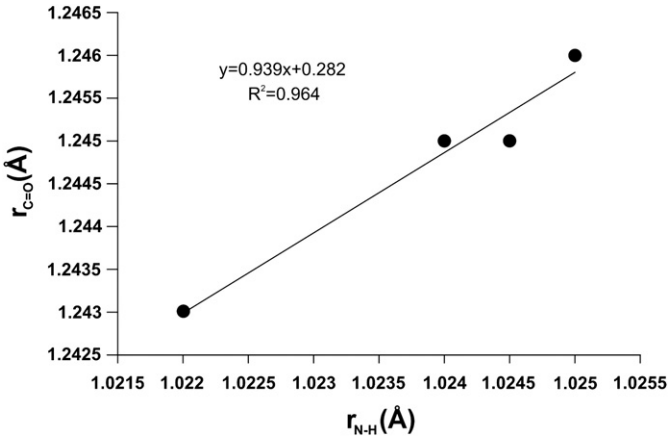

Fig. 2. Correlation of $r_{C=O}$ with r_{N-H} bond distance.

C═O bond distances can therefore serve as a good evidence for H-bond cooperativity in $(\alpha\text{-glygly})_{n=1-5}$ clusters. The calculated r_{C-N} bond length for central molecule in the pentamer model, 1.326 Å, differs from the isolated α-glygly by 0.005 Å. This value is in excellent agreement with available experimental data [32]. Furthermore, it is evident from Table 2 that intermolecular N–H···O═CNH, N–H···O═CO and C–H···O═CNH bond lengths are also notably changed by the cooperative nature of hydrogen bond. It is also seen that adding a third molecule considerably reduces $r_{N-H\cdots O=CNH}$ bond length by 0.215 Å. This distance decreases by 9% from dimer to pentamer. On the other hand, cooperative effects induce 0.142 and 0.078 Å reduction to N–H···O═CO and C–H···O═CNH bond length, respectively. Calculated cooperative effects in the geometry structure of α-glygly chain can be compared to other H-bonded systems. All the above results obtained for α-glygly clusters are compatible to those obtained at the DFT levels for formamide [51], N-methyl-formamide [52], acetamide [23], polyalanine chains in α-helical and extended structure and anti-parallel β-sheet models [53].

3.2. Binding energies

Table 3 presents the binding energies for optimized dimer α-glygly, provided by the three computational methods (B3LYP, $PW91_{XC}$ and MP2) with the 6-31+G*, 6-31++G**, cc-pVDZ and aug-cc-pVDZ basis sets. Results are consistent with other theoretical predictions. For example, the ΔE_e value from $PW91_{XC}$/6-31+G* (−57.457 kcal mol^{-1}) is consistent with B3LYP/D95** (−58.98 kcal mol^{-1}) value reported by Dannenberg et al. [16]. According to Table 3, various theories and basis sets produce different effects on the interaction energies. Investigating the basis set dependence reveals a decrease in the stabilization energy as the diffuse and polarization functions, for both 6-31+G* and cc-pVDZ basis sets, are concerned. However, B3LYP/6-31++G** calculations produce the smallest binding energies. It can be also observed from Table 3 that for the $(\alpha\text{-glygly})_2$ cluster, the BSSE corrected binding energies, ΔE_e^{CP}, are found to be −55.553, −57.007 and −58.391 kcal mol^{-1}, using the smallest basis set, at the B3LYP, $PW91_{XC}$ and MP2 levels, respectively. The

Table 3
Binding energies, ΔE_e, and BSSE corrected binding energies, ΔE_e^{CP}, for $(\alpha\text{-glygly})_2$ clusters[a].

Parameter	Method	6-31+G*	6-31++G**	cc-pVDZ	aug-cc-pVDZ
ΔE_e	B3LYP	−56.023	−55.673	−61.708	−56.756
	$PW91_{XC}$	−57.457	−56.763	−66.614	−58.045
	MP2	−59.381	−57.365	−68.325	−60.552
ΔE_e^{CP}	B3LYP	−55.553	−55.303	−61.188	−56.656
	$PW91_{XC}$	−57.007	−56.473	−66.034	−57.905
	MP2	−58.391	−57.025	−67.665	−60.352

[a] All calculated energies in kcal mol^{-1}.

Table 4
Calculated binding energies, ΔE_e, and BSSE corrected binding energies, ΔE_e^{CP}, with 6-311++G** basis set for $(glygl)_{n=2-5}$ clusters[a].

Parameter	Method	$n=2$	$n=3$	$n=4$	$n=5$
ΔE_e	B3LYP	−55.023	−62.132	−64.977	−65.022
	MP2	−61.241	−66.897	−69.884	−70.112
ΔE_e^{CP}	B3LYP	−54.962	−62.084	−64.714	−64.811
	MP2	−61.014	−66.852	−69.795	−69.893
Cooperativity	B3LYP	–	7.122	9.752	9.849
	MP2	–	5.838	8.781	8.879

[a] All calculated energies in kcal mol^{-1}.

data are about 3.427 kcal mol^{-1} smaller than the CP corrected interaction energy for peptide $(Gly_4)_2$ calculated at the B3LYP/D95** level [16]. On the other hand, stabilization energy of the dimer tends to decrease, by 0.25–1.366 kcal mol^{-1}, when a larger basis set (6-31++G**), containing second polarization and diffuse functions, is adopted. However, changing the cc-pVDZ basis set to aug-pVDZ produces a considerable difference in binding energy, about 8 kcal mol^{-1}, at the B3LYP and $PW91_{XC}$ levels. Furthermore, the effect of BSSE on the binding energies is quite selective. Since the BSSE introduces a nonphysical attraction between the monomers, the CP correction makes the chain less stable, which is observed to be larger for the MP2 calculations compared to the DFT methods.

For optimized linear α-glygly clusters, H-bonding interaction energies calculated at the MP2/6-311++G** and B3LYP/6-311++G** levels of theory, are presented in Table 4. The average binding

Table 5
Calculated ^{17}O NMR parameters (in ppm) for various α-glygly clusters.

Model	δ_{11}	δ_{22}	δ_{33}	δ_{iso}	$\Delta\delta$
Monomer	602.49	412.27	−62.54	317.41	427.63
Dimer	553.88	394.16	−41.19	302.28	377.40
	599.9	412.2	−68.15	314.65	427.88
Trimer	556	399.2	−38.06	305.71	375.43
	605.31	401.93	−69.41	312.61	439.05
	561.93	390.37	−32.91	306.46	383.20
Tetramer	556.94	389.09	−40.08	301.98	382.44
	557.56	400.88	−37.34	307.03	375.79
	556.51	390.14	−35.68	303.66	379.28
	617.51	406.06	−65.24	319.44	447.10
Pentamer	554.85	386.02	−39.82	300.35	381.75
	558.82	402	−39.99	306.94	377.82
	555.25	389.73	−34.63	303.45	377.70
	557.26	401.1	−38.45	306.64	375.94
	618.33	406.63	−65.38	319.86	447.71
Exp.[a]	546(562)	382(410)	−132(−108)	265.33(288)	421(411)

[a] Experimental ^{17}O NMR values for solid state α-glygly (polyglycine β-sheet) from Ref. [33].

Table 6
Calculated ^{15}N NMR parameters (in ppm) for various α-glygly clusters.

Model	δ_{11}	δ_{22}	δ_{33}	δ_{iso}	$\Delta\delta$
Monomer	261.87	92.75	64.89	139.84	183.05
Dimer	262.51	87.51	70.96	140.33	183.28
	263.94	95.78	73.04	140.25	179.53
Trimer	263.47	93.83	70.36	142.55	181.38
	262.11	90.52	69.72	140.78	181.99
	260.79	89.65	71.27	140.57	180.33
Tetramer	266.41	101.96	74.90	142.42	177.98
	264.35	90.90	72.06	142.44	182.87
	262.34	93.36	69.48	141.73	180.92
	263.26	92.14	70.67	142.02	181.86
Pentamer	260.82	88.59	71.55	140.32	180.75
	261.87	92.75	64.89	139.84	183.05
	272.44	104.45	75.25	150.71	182.59
	262.51	87.51	70.96	140.33	183.28
	265.94	98.78	74.04	146.25	179.53
Exp.[a]	220.80	79.70	46.80	115.80	157.55

[a] Experimental ^{15}N NMR values from Ref. [34].

energy deviation from dimer is another evidence for hydrogen-bond cooperativity. Both MP2 and B3LYP calculations predict an increase in cooperative effects for α-glygly clusters. Cooperative enhancement stabilizes the average H-bond interaction in the pentamer by about −64.811 and −69.893 kcal mol^{-1}, at the B3LYP and MP2 levels, which is equivalent to adding 9.849 and 8.879 kcal mol^{-1} to the dimer H-bonding energy, respectively. The ΔE_e is increased by 18% at the B3LYP and 15% at the MP2 levels of theories, which is smaller than the extrapolated percent in one dimensional chains of formamide (200%) [51] and urea molecules (55%) [27].

3.3. NMR chemical shift tensors

Tables 5 and 6 show the ^{17}O and ^{15}N chemical shift eigenvalues and their associated isotropy and anisotropy values for various $(\alpha\text{-glygly})_{n=1-5}$ clusters calculated at the B3LYP/6-311++G** level. Besides, available experimental ^{17}O and ^{15}N NMR data [33,34] are also tabulated in order to validate of our calculated data. It has been extensively reported [54,55] that down-shift of the ^{17}O and ^{15}N chemical shift isotropy value involved in the N–H···O═CNH hydrogen-bonded systems generally increases with the H-bonded cluster size; which is a reflection of cooperative effect. Therefore, displacement in ^{17}O and ^{15}N NMR isotropy values is always an indicator of the nature of cooperativity.

The intermolecular interactions are expected to strongly affect electronic environment at the hydrogen-bonded nuclei. Thus, the cooperative effects in electronic structure induced by N–H···O═CNH, N–H···O═CO and C–H···O═CNH hydrogen-bond formations influence the chemical shift of the ^{17}O nuclei in $(\alpha\text{-glygly})_{2-5}$ clusters. According to the B3LYP/6-311++G** calculations (Table 5), the calculated δ_{11} value decreases for all interior molecules in the $(\alpha\text{-glygly})_{1-5}$ clusters. The calculated $\delta_{11}(^{17}O)$ value for central molecule in pentamer cluster is 555.25 ppm which differs from the monomer by 47.24 ppm. Although the calculated δ_{11} value for this model deviates slightly from their experimental counterparts (546 ppm) [33], the agreement is still good considering the uncertainties in experiment and theory. For the intermediate component, δ_{22}, the magnitude of these changes is found to be 22.54 ppm, though the shift change is relatively large from tetramer to pentamer cluster. On the other hand, the $\delta_{iso}(^{17}O)$ value decreases from 317.41 ppm for the monomer to 303.45 ppm for the central molecule in pentamer; while the associated anisotropy parameter increases from −332.52 to −294.94 ppm. By increasing

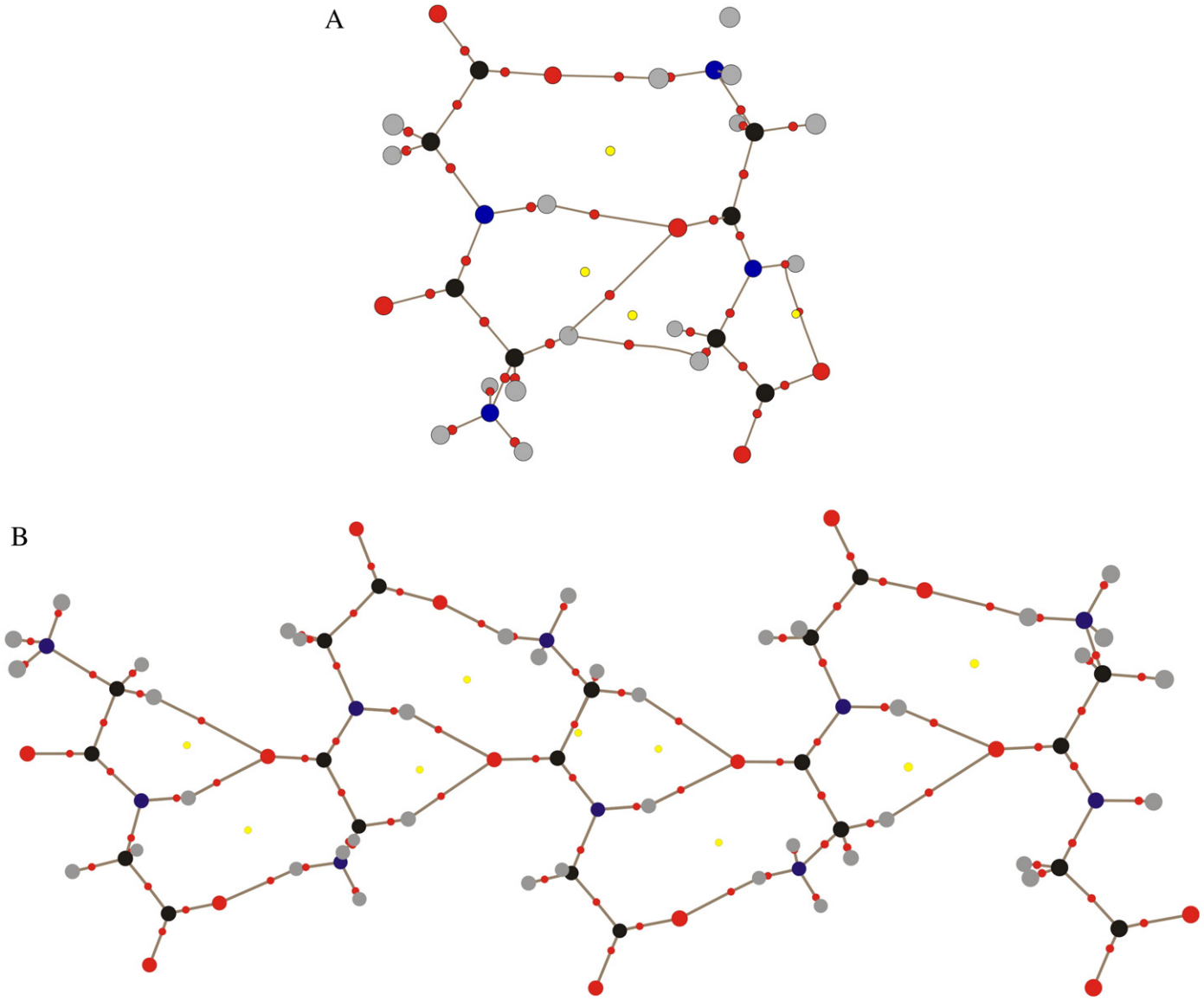

Fig. 3. Molecular graphs of the fully optimized systems: (A) dimer and (B) pentamer cluster. Graphs were obtained at the B3LYP/6-311++G** level. Big circles correspond to attractors and small ones to critical points.

Table 7
Topological parameters for the optimized system analyzed here[a].

Interaction	Model	ρ_C	$\nabla^2\rho_C$	K_C	V_C	H_C	$-\frac{K_C}{V_C}$
N–H···O═CO	Dimer	0.0262	0.1055	0.0028	−0.0321	−0.0293	0.087
	Trimer	0.0312	0.1231	0.0023	−0.0369	−0.0346	0.062
	Tetramer	0.0338	0.1375	0.0021	−0.0385	−0.0364	0.055
	Pentamer	0.0417	0.1692	0.0003	−0.0423	−0.0420	0.007
N–H···O═CNH	Dimer	0.0143	0.0532	0.0021	−0.0174	−0.0153	0.121
	Trimer	0.0211	0.0589	0.0024	−0.0247	−0.0223	0.097
	Tetramer	0.0214	0.0927	0.0026	−0.029	−0.0264	0.090
	Pentamer	0.0215	0.0933	0.0028	−0.0318	−0.0290	0.088
C–H···O═CNH	Dimer	0.0083	0.0213	0.0008	−0.0037	−0.0029	0.216
	Trimer	0.0091	0.0301	0.0014	−0.0072	−0.0058	0.194
	Tetramer	0.0098	0.0341	0.0015	−0.0114	−0.0099	0.132
	Pentamer	0.0099	0.0363	0.0015	−0.0119	−0.0104	0.126

[a] All, ρ_C, $\nabla^2\rho_C$, K_C, V_C and H_C values in atomic unit.

the cluster size, from dimer to pentamer cluster, the chemical shift eigenvalues reach a limit. This indicates that, in agreement with the previous sections, the cooperative effects on ^{17}O chemical shift tensor decrease by increasing the number of monomers in the clusters.

Experimentally obtained accurate magnitudes of the principal components of the ^{17}O NMR tensors of α-glygly and polyglycine (β-sheet) enabled the examination of the accuracy of our calculated values. As Table 5 indicates, all calculated values for central molecule in pentamer cluster are in significant agreement with experimental values with the exception of $\delta_{33}(^{15}N)$ component. It should be noted that NMR parameters primarily depend on the local chemical bonding environment, within a few Å of the nucleus under consideration. Thus, to make an accurate description of NMR chemical shielding of hydrogen-bonded systems, high quality basis sets is really demanding. Based on the theoretical calculations, Oldfield et al. [56] concluded that basis set size primarily affects the absolute shielding and very good correlations can he obtained simply by including slightly larger basis sets on a small number of selected atoms. Assuming a correct starting geometry, there are three sources of errors that may cause the DFT method to falter and to predict incorrect ^{17}O chemical shifts. The first is an insufficient basis set. In particular, the diffuse functions left out for reasons of computational efficiency in the calculations of ^{17}O chemical shielding tensors. The second source of error is improper inclusion of intermolecular interactions. Since the linear H-bonding network was included for α-glygly, only the effect of long-range electrostatic interactions must be considered. The final possible defect is the improper incorporation of electron correlation effects. Although a detailed study is missing, an incorrect isotropic radial dependence of the electron density presumably would have a much smaller effect on the orientation of the ^{17}O chemical shielding tensor than on the magnitude of the principal elements of chemical shielding tensor.

^{15}N NMR chemical shift values calculated for various α-glygly clusters are compared in Table 6. As evident from Table 6, the calculated ^{15}N chemical shift values at the amide site exhibit a rather strong dependency on cooperative effects. This is consistent with the $\delta_{iso}(^{15}N)$ increasing by the cooperative effects [53]. The results also show a noticeable increasing of the principal components from the monomer to the central molecule in pentamer: $\Delta\delta_{11} = 10.87$ ppm, $\Delta\delta_{22} = 11.70$ ppm, and $\Delta\delta_{33} = 10.36$ ppm. The calculated average δ_{iso} (^{15}N) values per cluster are as follows: 140.29, 141.30, 142.15 and 143.49 ppm, which means an increase of 3% with the greatest jump of 1.36 ppm from tetramer to pentamer. In addition, the magnitudes of calculated $\delta_{ii}(^{15}N)$ components, isotropic and anisotropic values are generally underestimated for central molecule in pentamer cluster.

3.4. Atoms in Molecules analyses

Bader theory is applied here to analyze the characteristics of N–H···O and C–H···O bond critical points (BCP). In the equilibrium geometry, an interatomic interaction line is regarded as bond path [48]. For such an equilibrium molecular structure, there is a virial path for each bond path of interacting atoms [57].

Molecular graphs of optimized dimer and pentamer α-glygly clusters are depicted in Fig. 3. For N–H···O═CNH, N–H···O═CO, and C–H···O═CNH interactions, there are corresponding bond paths and critical points (CPs) within the equilibrium structures. As indicated in previous studies, characteristics of proton···acceptor BCPs are very useful to estimate the cooperative effects in hydrogen-bonded systems [58]. Parameters such as electron density at the proton···acceptor BCP (ρ_C) and its Laplacian ($\nabla^2\rho_C$) often correlate with the H-bond energy or other parameters, like proton···acceptor distance, the proton donating bond length, and etc. [48]. As presented in Fig. 3, there are specific bond paths and BCPs for every N–H···O═CNH, N–H···O═CO and C–H···O═CNH connections. Therefore, the first topological criterion of the existence of H-bonding interaction is fulfilled. As in Table 7, the calculated electron densities at N–H···O═CO, N–H···O═CNH, and C–H···O═CNH bond critical points are found to be 0.0262, 0.0143 and 0.0083 a.u. in dimer system, respectively. These values increase by 59.6, 50.35 and 19.3% by moving from dimer to pentamer, respectively. A 0.064 a.u. increase is observed for corresponding $\nabla^2\rho(r_{cp})$ values of N–H···O═CO, which is larger than those of N–H···O═CNH (0.040 a.u.) and C–H···O═CNH (0.015 a.u.) for the same clusters. The order of cooperativity enhancement in ρ and $\nabla^2\rho(r_{cp})$, calculated for α-glygly clusters, supports the fact that degree of cooperativity is proportional to the strength of hydrogen bond.

As also evident from Table 7, cooperative effects tend to increase the total electron density value, H_C, of all intermolecular interactions. For pentamer cluster, the calculated H_C values N–H···O═CO, N–H···O═CNH, and C–H···O═CNH interactions are found to be −0.0420, −0.0290 and −0.0104 a.u., respectively. It was claimed that, in case of positive $\nabla^2\rho(r_{cp})$ and negative H_C, the H-bonding interaction is partly covalent in nature [59]. H_C is the electron energy density at BCP, which is equal to the sum of kinetic electron energy density (K_C) and potential electron energy density (V_C). The latter value is negative, and the previous one is positive. The balance between those two values determines the nature of interaction. Therefore, the characteristics of $-K_C/V_C$ may define covalent and noncovalent interactions. For linear

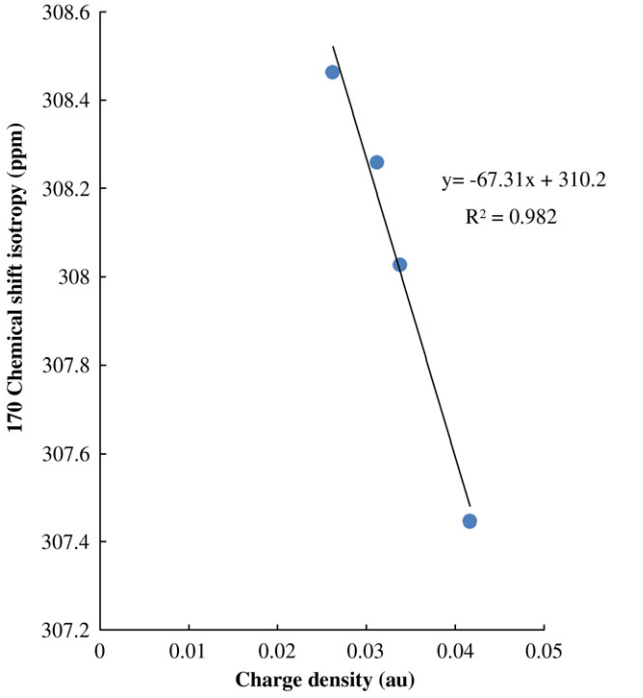

Fig. 4. Correlation of calculated ^{17}O chemical shielding isotropy values with charge density at N–H···O═CNH bond critical point.

α-glygly clusters, one can observe all tendencies, indicating the role of cooperative effect: an increase in N–H···O interaction and H_C amount and a decrease in $-K_C/V_C$ as the number of α-glygly molecules increases. Similar tendencies are observed for C–H···O interaction (Table 7). However, in the former case, all N–H···O interactions may be treated more covalent in nature than C–H···O, as the H_C values are more negative.

Fig. 4 shows the dependency of ^{17}O chemical shift isotropy to the electron density at the corresponding N–H···O═CNH bond critical points. The obtained linear correlation coefficient is equal to 0.982. This correlation indicates that the two representations of N–H···O═CNH strengths, based upon NMR and AIM approaches, are approximately equivalent. Thereby, regarding the cooperativity of N–H···O═CNH interaction, it is believed that the capacity of the linear α-glygly clusters to concentrate electrons at the N–H···O BCP is sensitive to the cluster size. Hence, the average value of ρ_C (0.0215 a.u.) for the pentamer is 1.5 times greater than that for the dimer (0.0143 a.u.).

4. Conclusion

The influence of cooperativity effect on N–H···O═CNH, N–H···O═CO, and C–H···O═CNH was investigated for $(\alpha\text{-glygly})_{1-5}$ clusters. It is understood that the equilibrium geometries and interaction energies of dimer α-glygly depend considerably on the level of theory. For trimer cluster, more stability, 7.109 kcal mol^{-1}, was obtained at the B3LYP/6-311++G** level of theory, due to formation of the second hydrogen bond. Our calculations indicated that, as cluster size increases, the calculated ^{17}O chemical shift isotropy values shift to lower values. Furthermore, the capacity of α-glygly clusters to concentrate electrons at the N–H···O═CNH, N–H···O═CO, and C–H···O═CNH BCP increases with the cluster size. Such cooperative effects help rationalize the common occurrence of similar H-bonding interactions in biosystems.

References

[1] M.J. Elrodt, R.J. Saykally, Many-body effects in intermolecular forces, Chem. Rev. 94 (1994) 1975–1997.
[2] J.E. Del Bene, J.A. Pople, Intermolecular energies of small water polymers, Chem. Phys. Lett. 4 (1969) 426–428.
[3] A. Van der Vaart, K.M. Merz, Charge transfer in biologically important molecules: comparison of high-level ab initio and semiempirical methods, Int. J. Quantum Chem. 77 (2000) 27–43.
[4] L. Rincon, R. Almeida, D.G. Aldea, Many-body energy decomposition analysis of cooperativity in hydrogen flouride clusters, Int. J. Quantum Chem. 102 (2005) 443–453.
[5] E. Clementi, W. Kolos, G.C. Lie, G. Ranghino, Nonadditivity of interaction in water trimers, Int. J. Quantum Chem. 17 (1980) 377–398.
[6] J.F. Gaw, Y. Yamaguchi, M.A. Vincent, H.F. Schaefer III, Vibrational frequency shifts in hydrogen-bonded systems: the hydrogen fluoride dimer and trimer, J. Am. Chem. Soc. 106 (1988) 3133–3138.
[7] R. Ludwig, F. Weinhold, T.C. Farrar, Structure of liquid N-methylacetamide: temperature dependence of NMR chemical shifts and quadrupole coupling constants, J. Phys Chem., A 101 (1997) 8861–8870.
[8] R. Ludwig, F. Weinhold, T.C. Farrar, Theoretical study of hydrogen bonding in liquid and gaseous N-methylformamide, J. Chem. Phys. 107 (1997) 499–507.
[9] S. Suhai, Cooperative effects in hydrogen-bonding 4th-order many body perturbation theory studies of water oligomers and of an infinite water chain as a model for ice, J. Chem. Phys. 101 (1994) 9766–9782.
[10] Q.Y. Xia, H.M. Xiao, X.H. Ju, X.D. Gong, DFT study on cooperativity in the interactions of hydrazoic acid clusters, Int. J. Quantum Chem. 94 (2003) 279–286.
[11] H. Tan, W. Qu, G. Chen, R. Liu, The role of charge transfer in the hydrogen bond cooperative effect of cis-N-methylfortnamide oligomers, J. Phys. Chem., A 109 (2005) 6303–6317.
[12] T. van Mourik, A.J. Dingley, Characterizing the cooperativity in H-bonded amino structures, J. Phys. Chem., A 111 (2007) 11350–11358.
[13] B.F. King, F. Weinhold, Structure and spectroscopy of (HCN)*n* clusters-cooperative and electronic delocalization effects in C–H…N hydrogen-bonding, J. Chem. Phys. 103 (1995) 333–347.
[14] B.F. King, T.C. Farrer, F. Weinhold, Quadrupole coupling constants in linear $(HCN)_n$ clusters: theoretical and experimental evidence for cooperativity effects in C–H…N hydrogen bonding, J. Chem. Phys. 103 (1995) 348–352.
[15] N. Kobko, L. Paraskevas, E. del Rio, J.J. Dannenberg, Cooperativity in amide hydrogen bonding chains: implications for protein-folding models, J. Am. Chem. Soc. 123 (2001) 4348–4349.
[16] R. Viswanathan, A. Asensio, J.J. Dannenberg, Cooperative hydrogen-bonding in models of antiparallel β-sheets, J. Phys. Chem., A 108 (2004) 9205–9212.
[17] T. Kar, S. Scheiner, Comparison of cooperativity in CH···O and OH···O hydrogen bonds, J. Phys. Chem., A 108 (2004) 9161.
[18] G.A. Jeffrey, An Introduction to Hydrogen Bonding, Oxford University Press, New York, 1997.
[19] S.W. Hunt, K.J. Higgins, M.B. Craddock, C.S. Brauer, K.R. Leopold, Influence of a polar near-neighbor on incipient proton transfer in a strongly hydrogen bonded complex, J. Am. Chem. Soc. 125 (2003) 13850–13860.
[20] S. Scheiner, Hydrogen Bonding: a Theoretical Perspective, Oxford University Press, New York, 1997 1997.
[21] T. Kar, S. Scheiner, Comparison between hydrogen and dihydrogen bonds among H_3BNH_3, H_2BNH_2, and NH_3, J. Chem. Phys. 119 (2003) 1473–1482.
[22] M.D. Esrafili, H. Behzadi, N.L. Hadipour, ^{14}N and ^{17}O electric field gradient tensors in benzamide clusters: theoretical evidence for cooperative and electronic delocalization effects in N–H···O hydrogen bonding, Chem. Phys. 348 (2008) 175–180.
[23] M.D. Esrafili, H. Behzadi, N.L. Hadipour, Theoretical study of N–H···O hydrogen bonding properties and cooperativity effects in linear acetamide clusters, Theor. Chem. Acc. 121 (2008) 135–146.
[24] A. Karpfen, E.S. Kryachko, Strongly blue-shifted C–H stretches: interaction of formaldehyde with hydrogen fluoride clusters, J. Phys. Chem., A 109 (2005) 8930–8937.
[25] D.B. DuPré, C. Yappert, Cooperative hydrogen- and π H-bonded interactions involving water and the ethylenic double bond, J. Phys. Chem., A 106 (2002) 567–574.
[26] C. Rovira, J.J. Novoa, A density functional study of crystalline acetic acid and its proton transfer polymorphic forms, J. Chem. Phys. 113 (2000) 9208–9216.
[27] N. Kobko, J.J. Dannenberg, Cooperativity in amide hydrogen bonding chains. Relation between energy, position, and H-bond chain length in peptide and protein folding models, J. Phys. Chem. A 107 (2003) 10389–10395.
[28] A. Masunov, J.J. Dannenberg, Theoretical study of urea and thiourea. 2. Chains and ribbons. J. Phys. Chem. B 104 (2000) 806–810.
[29] A.R. Ghaderi, H. Sabzyan, N.L. Hadipour, Correlation between NQR parameters and residue size of aliphatic amino acids and their dimers, Biophys. Chem. 120 (2006) 62–70.
[30] J. Birn, A. Poon, Y. Mao, A. Ramamoorthy, Ab initio study of $^{13}C_\alpha$ chemical shift anisotropy tensors in peptides, J. Am. Chem. Soc. 126 (2004) 8529–8534.
[31] F. Elmi, N.L. Hadipour, A study on the intermolecular hydrogen bonds of α-glycylglycine in its actual crystalline phase using ab initio calculated ^{14}N and ^{2}H nuclear quadrupole coupling constants, J. Phys. Chem. A 109 (2005) 1729–1733.
[32] S.A. Moggach, D.R. Allan, S. Parsons, L. Sawyer, Effect of pressure on the crystal structure of aglycylglycine to 4.7 GPa; application of Hirshfeld surfaces to analyze contacts on increasing pressure, Acta Crystallogr. B62 (2006) 310–320.
[33] T. Kameda, N. Takeda, S. Ando, I. Ando, D. Hashizume, Y. Ohashi, Structure of glygly peptide in structure of glygly peptide in studied by X-ray diffraction and solid state ^{13}C-NMR methods, Biopolymers 45 (1998) 333–339.
[34] S. Kuroki, A. Takahashi, I. Ando, A. Shoji, T. Ozaki, Hydrogen-bonding structural study of solid peptides and polypeptides containing a glycine residue by ^{17}O NMR spectroscopy, J. Mol. Struct. 323 (1994) 197–208.
[35] D.K. Lee, R.J. Wittebort, A. Ramamoorthy, Characterization of ^{15}N chemical shift and ^{1}H–^{15}N dipolar coupling interactions in a peptide bond of uniaxially oriented and polycrystalline samples by one-dimensional dipolar chemical shift solid-state NMR spectroscopy, J. Am. Chem. Soc. 120 (1998) 8868–8874.
[36] I. Ando, T. Kameda, N. Asakawa, S. Kuroki, H. Kurosu, Structure of peptides and polypeptides in the solid state as elucidated by NMR chemical shift, J. Mol. Struct. 441 (1998) 213–230.
[37] M.J. Frisch, G.W. Trucks, H.B. Schlegel, G.E. Scuseria, M.A. Robb, J.R. Cheeseman, V.G. Zakrzewski, J.A. Montgomery, R.E. Stratmann, J.C. Burant, S. Dapprich, J.M. Millam, A.D. Daniels, K.N. Kudin, M.C. Strain, O. Farkas, J. Tomasi, V. Barone, M. Cossi, R. Cammi, B. Mennucci, C. Pomelli, C. Adamo, S. Clifford, J. Ochterski, G.A. Petersson, P.Y. Ayala, Q. Cui, K. Morokuma, D.K. Malick, A.D. Rabuck, K. Raghavachari, J.B. Foresman, J. Cioslowski, J.V. Ortiz, A.G. Baboul, B.B. Stefanov, G. Liu, P. Liashenko APiskorz, I. Komaromi, R. Gomperts, R.L. Martin, D.J. Fox, T. Keith, M.A. Al-Laham, C.Y. Peng, A. Nanayakkara, C. Gonzalez, M. Challacombe, P.M.W. Gill, B. Johnson, W. Chen, M.W. Wong, J.L. Andres, C. Gonzalez, M. Head-Gordon, E.S. Replogle, J.A. Pople, Gaussian 98, Gaussian Inc., Pittsburgh, P B, 1998.
[38] S.F. Boys, F. Bernardi, The calculation of small molecular interactions by the differences of separate total energies. Some procedures with reduced errors, Mol. Phys. 19 (1970) 553–566.
[39] P. Salvador, M.M. Szczesniak, Counterpoise-corrected geometries and harmonic frequencies of N-body clusters: application to $(HF)_n$ ($n=3,4$), J. Chem. Phys. 118 (2003) 537–549.
[40] J.J. Novoa, C. Sosa, Evaluation of the density functional approximation on the computation of hydrogen bond interactions, J. Phys. Chem. 99 (1995) 15873–15878.
[41] K. Wolinski, J.F. Hilton, P. Pulay, Efficient implementation of the gauge-independent atomic orbital method for NMR chemical shift calculations, J. Am. Chem. Soc. 112 (1990) 8251–8260.
[42] M.D. Esrafili, F. Elmi, N.L. Hadipour, Density functional theory investigation of hydrogen bonding effects on the oxygen, nitrogen and hydrogen electric field gradient and chemical shielding tensors of anhydrous chitosan crystalline structure, J. Phys. Chem., A 111 (2007) 963–970.
[43] R. Ida, M. De Clerk, G. Wu, Influence of N–H···O and C–H···O Hydrogen Bonds on the ^{17}O NMR tensors in crystalline uracil: computational study, J. Phys. Chem., A 110 (2006) 1065–1071.
[44] M.J. Duer, Solid State NMR Spectroscopy, Blackwell Science Ltd., London, 2002.

[45] R.E. Wasylishen, D.L. Bryce, A revised experimental absolute magnetic shielding scale for oxygen, J. Chem. Phys. 117 (2002) 10061–10066.
[46] C.J. Jameson, A.K. Jameson, D. Oppusunggu, S. Wille, P.M. Burrell, J.J. Mason, ^{15}N nuclear magnetic shielding scale from gas phase studies, J. Chem. Phys. 74 (1981) 81–88.
[47] F. Biegler-Konig, J. Schonbohm, D. Bayles, Software news and updates – AIM2000 – a program to analyze and visualize atoms in molecules, J. Comput. Chem. 22 (2001) 545–559.
[48] R.F.W. Bader, Atoms in Molecules—a Quantum Theory, Oxford University Press, New York, 1990.
[49] J.D. Bernal, The crystal structure of the natural amino acids and related compounds, Z. Kristallogr. Kristallgeom. Kristallphys. Kristallchem. 78 (1931) 363–369.
[50] S.J. McGlone, P.S. Elmes, R.D. Brown, P.D. Godfrev, Molecular structure of a conformer of glycine by microwave spectroscopy, J. Mol. Struct. 485–486 (1999) 225–238.
[51] R. Vargas, J. Garza, R.A. Friesner, H. Stern, B.P. Hay, D.A. Dixon, Strength of the N–H···O═C and C–H···O═C bonds in formamide and N-methylacetamide dimers, J. Phys. Chem., A 105 (2001) 4963–4968.
[52] A.G. Martínez, E.T. Vilar, G. Fraile, P. Martínez-Ruiz, Density functional study of self-association of n-methylformamide and its effect on intramolecular and intermolecular geometrical parameters and cis/trans population, J. Chem. Phys. 124 (2006) 234305–234310.
[53] R. Wieczorek, J.J. Dannenberg, H-bonding cooperativity and energetics of α-helix formation of five 17-amino acid peptides, J. Am. Chem. Soc. 125 (2003) 8124–8129.
[54] K. Yamada, S. Dong, G. Wu, Solid-state ^{17}O NMR investigation of the carbonyl oxygen electric-field-gradient tensor and chemical shielding tensor in amides, J. Am. Chem. Soc. 122 (2000) 11602–11609.
[55] M. Tafazzoli, S.K. Amini, A survey of hydrogen bonding in imidazole and its 4-nitro derivative by ab initio and DFT calculations of chemical shielding, Chem. Phys. Lett. 431 (2006) 421–427.
[56] D.D. Laws, H. Le, A.C. De Dios, R.H. Havlin, E. Oldfield, A basis size dependence study of carbon-13 nuclear magnetic resonance spectroscopic shielding in alanyl and valyl fragments: toward protein shielding hypersurfaces, J. Am. Chem. Soc. 117 (1995) 9542–9546.
[57] T.A. Keith, R.F.W. Bader, Y. Aray, Structural homeomorphism between the electron density and the virial field, Int. J. Quantum Chem. 57 (1996) 183–198.
[58] O. Mo, M. Yánez, J.J. Elguero, Cooperative (nonpairwise) effects in water trimers: an ab initio molecular orbital study, J. Chem. Phys. 97 (1992) 6628–6638.
[59] S. Jenkins, I. Morrison, The chemical character of the intermolecular bonds of seven phases of ice as revealed by ab initio calculation of electron densities, Chem. Phys. Lett. 317 (2000) 97.